Biomolecular Sensing Using Near-Null Single Wavelength Arrayed Imaging Reflectometry

ARTICLE *in* ANALYTICAL CHEMISTRY · OCTOBER 2006

Impact Factor: 5.64 · DOI: 10.1021/ac0609226 · Source: PubMed

3 AUTHORS, INCLUDING:

Tingjuan Gao
University of California, Davis
25 PUBLICATIONS **89** CITATIONS

SEE PROFILE

Article

Biomolecular Sensing Using Near-Null Single Wavelength Arrayed Imaging Reflectometry

Tingjuan Gao, Jinghui Lu, and Lewis J. Rothberg

Anal. Chem., **2006**, 78 (18), 6622-6627• DOI: 10.1021/ac0609226 • Publication Date (Web): 12 August 2006

Anal. Chem. **2006,** *78,* 6622−6627

Biomolecular Sensing Using Near-Null Single Wavelength Arrayed Imaging Reflectometry

Tingjuan Gao, Jinghui Lu, and Lewis J. Rothberg*

Department of Chemistry, Department of Chemical Engineering, Center for Future Health, University of Rochester, Rochester, New York 14627

We use reflectivity changes at an interface functionalized with molecular probes to detect label-free biomolecular binding. Attachment of the target molecules to the surface alters the effective thickness of an antireflective coating formed by thermal oxidation of a silicon wafer to remove destructive interference of the reflected waves. The thermal oxide thickness is adjusted for precise interference using electrostatic layer-by-layer self-assembly of polyelectrolytes to which the molecular probes can be bound covalently. Reflectivity increases of over a factor of 100 are observed for binding of 2.5 nm of streptavidin to biotinylated polyelectrolytes, considerably more sensitive than surface plasmon resonance detection. Theoretical modeling is in agreement with the experimentally observed reflectivity increases and suggests the sensitivity is at present limited by the roughness of the oxide.

Development of sensitive label-free platforms to detect biomolecules has facilitated biochemical research. The most widely used approach is surface plasmon resonance (SPR),[1,2] which is typically sensitive to adsorption of only a few angstroms of material, but remains relatively expensive, has limited dynamic range, and is difficult to interpret quantitatively. Ellipsometry[3,4] and interferometric methods that detect spectral shifts[5−11] are both very sensitive but expensive to implement, particularly if imaging of probe arrays is desired. We recently reported a simplified version of these that exploits conditions of nearly perfect destructive interference in reflectivity that can be achieved when the wavelength and incidence angle can be controlled precisely. We demonstrated the approach on submonolayer detection of DNA[12] and refer to it as reflective interferometry (RI).

The near-null detection provides high sensitivity, excellent dynamic range, and the ability to infer the amount of target adsorbed quantitatively but requires a tunable source to provide a good match to the optical thickness of the interference coating. Implementation with a lamp and spectrometer is, however, bulky and expensive, also providing relatively poorly defined incidence angle and large spectral bandwidth that limit the sensitivity. Here we report a single-color variation with a highly collimated and monochromatic laser that results in the ability to detect average adsorption of less than 1.2 Å. The apparatus is amenable to very inexpensive construction and could be made small and portable.

We demonstrate control of the thickness of the interference coating using layer-by-layer electrostatic self-assembly of polyelectrolytes[13−15] applied to optimize the thickness for use with a HeNe laser. Functional groups on the polyelectrolytes also serve as suitable binding sites for probes with molecular recognition capability. The efficacy of the platform is demonstrated with well-documented biotin−streptavidin chemistry. Reflectivity changes larger than a factor a 10 are observed for binding 3 Å of biotin on the polyelectrolytes and nearly a factor of 100 when binding less than 3 nm of streptavidin to the biotin. We show that these measurements are in quantitative agreement with theoretical predictions that include nonidealities associated with imperfect surface roughness. Theoretical comparison with optimized SPR based on literature geometry[16−18] results suggests that this implementation of reflective interferometry is considerably more sensitive than SPR.

EXPERIMENTAL SECTION

Materials. Nominally undoped silicon wafers with thermally grown oxides of 134 nm were obtained from the Microelectronics Center at the Rochester Institute of Technology. Poly(allylamine hydrochloride) (PAH; average MW 70 000 Aldrich), poly(sodium

* Corresponding author. Voice: 585-273-4725. Fax: 585-206-0205. E-mail: rothberg@chem.rochester.edu.

(1) Smith, E. A.; Corn, R. M. *Appl. Spectrosc.* **2003**, *57* (11), 320A−332A.
(2) Homola, J.; Yee, S. S.; Gauglitz, G. *Sens. Actuators, B: Chem.* **1999**, *54* (1−2), 3−15.
(3) Arwin, H. *Thin Solid Films* **2000**, *377*, 48−56.
(4) Arwin, H. *Thin Solid Films* **1998**, *313*, 764−774.
(5) Brecht, A.; Ingenhoff, J.; Gauglitz, G. *Sens. Actuators, B: Chem.* **1992**, *6* (1−3), 96−100.
(6) Lin, V. S. Y.; Motesharei, K.; Dancil, K. P. S.; Sailor, M. J.; Ghadiri, M. R. *Science* **1997**, *278* (5339), 840−843.
(7) Jenison, R.; Yang, S.; Haeberli, A.; Polisky, B. *Nat. Biotechnol.* **2000**, *19*, 62−65.
(8) Chan, S.; Li, Y.; Rothberg, L. J.; Miller, B. L.; Fauchet, P. M. *Mater. Sci. Eng. C* **2001**, *15*, 277−282.
(9) Pan, S.; Rothberg, L. J. *Nano Lett.* **2003**, *3* (6), 811−814.
(10) Pacholski, C.; Sartor, M.; Sailor, M. J.; Cunin, F.; Miskelly, G. M. *J. Am. Chem. Soc.* **2005**, *127*, 11636−11645.
(11) Gauglitz, G. *Anal. Bioanal. Chem.* **2005**, *381*, 141−155.
(12) Lu, J.; Strohsahl, C. M.; Miller, B. L.; Rothberg, L. J. *Anal. Chem.* **2004**, *76* (15), 4416−4420.
(13) Decher, G.; Hong, J.; Schmitt, J. *Thin Solid Films* **1992**, *210* (1−2), 831−835.
(14) Ferreira, M.; Rubner, M. F. *Macromolecules* **1995**, *28* (21), 7107−7114.
(15) Shiratori, S. S.; Rubner, M. F. *Macromolecules* **2000**, *33*, 4213−4219.
(16) Nelson, B. P.; Frutos, A. G.; Brockman, J. M.; Corn, R. M. *Anal. Chem.* **1999**, *71*, 3928−3934.
(17) Jordan, C. E.; Frutos, A. G.; Thiel, A. J.; Corn, R. M. *Anal. Chem.* **1997**, *69*, 4939−4947.
(18) Wark, A. W.; Lee, H. J.; Corn, R. M. *Anal. Chem.* **2005**, *77* (13), 3904−3907.

10.1021/ac0609226 CCC: $33.50
Published on Web 08/12/2006

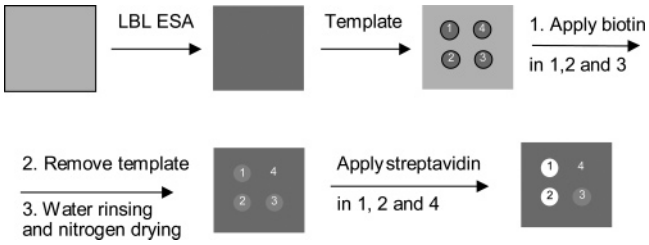

Figure 1. Wafer treatment procedure. The interference coating thickness is adjusted by polyelectrolyte self-assembly. A template is applied to create four distinct spots. Biotin receptors are attached to spots 1, 2, and 3 while spot 4 is left bare as a control. Streptavidin solution is applied to spots 1, 2, and 4. Spot 3 is used to measure biotin thickness while spot 4 is used as a control to measure nonspecific binding of streptavidin.

4-polystyrenesulfonate) (SPS; average MW 70 000 Aldrich), poly(acrylic acid) (PAA; average MW 100 000 Aldrich), *N*-hydroxysuccinimide (NHS, Fluka), *N*-(3-dimethylaminopropyl)-*N*′-ethylcarbodiimide hydrochloride (EDC; Sigma), biotin ethylenediamine (Biotium, Inc.), and streptavidin (Sigma) were used as received. Millipore-filtered water was used for all aqueous solutions and rinsing.

Layer-by-Layer Electrostatic Self-assembly (LBL ESA). Silicon wafers were diced into pieces of 2 cm × 4 cm dimensions to be used as substrates. These were cleaned for 1 h in boiling piranha solution, freshly prepared by mixing 3 volumes of 30% hydrogen peroxide and 7 volumes of 98% sulfuric acid. The substrates were rinsed repeatedly with water and dried under flowing nitrogen gas. Bilayers of charged polyelectrolytes were applied with a robotic HMS Programmable Slide Stainer (Carl Zeiss Inc.). Substrates were immersed into PAH solution (0.01 M, pH 6.42) for 10 min, followed by immersion while agitating in three separate bins of water for 2, 1, and 1 min, respectively. The substrates were then immersed into SPS solution (0.01 M, pH 6.40) for 10 min followed by an identical rinse procedure. This protocol was repeated by a predetermined number of cycles as needed to augment the effective thickness of the antireflection coating on the silicon wafer. For the final layer on the substrate, PAA solution (0.01 M, pH 2.96) was used instead of PAH to produce relatively dense carboxylate groups for the biomolecular probe attachment chemistry. After completion of the polyelectrolyte layers, the substrates were dried in an oven (100 °C) for 1 h.

Ellipsometric Measurements. The overlayer thicknesses on the silicon substrates were determined before and after layer-by-layer deposition by spectroscopic ellipsometry (JL Woollam M-2000). We used the silicon oxide refractive index from the literature and assumed the refractive index of the multilayer films to be 1.55 at 632 nm for modeling the ellipsometric data.

Surface Attachment Chemistry and Experimental Design for Streptavidin Detection. The steps involved in the preparation of the chips are summarized in Figure 1. After LBL ESA, an elastomeric cover with patterned wells was used to mask the substrate so that different chemistry could be applied at different spatial locations. It was used to generate a pattern of four chemically distinct spots while the remainder of the substrate was untreated. Spots 1, 2, and 3 were then modified by applying 1.0 μL of a mixture of equal volumes of EDC (31 mM) and NHS (7.8 mM) along with 1.0 μL of 0.14 M biotin ethylenediamine in 4-morphilineethanesulfonic acid (MES) buffer solution (pH 6.5) for 8 h. The elastomeric template was then removed, and the substrate was rinsed with water and dried under flowing nitrogen gas. Streptavidin (0.25 mg/mL in 10 mM PBS, pH 7.4) was applied to two of the three biotinylated spots (1 and 2) and to the untreated spot (4) for 45 min to assess both specific and nonspecific binding. This procedure necessitates careful placement of the analyte drop so that it registers with the underlying probe spots. We found that this was possible to do by hand when the positions of the spots were marked ruled lines on graph paper below the chip. Fortunately, the analyte drops did not spread significantly after being applied to the surface. Again, this was followed by rinsing with water and drying under flowing nitrogen gas.

Single-Color RI Measurement. The reflectivity of a collimated HeNe laser was measured for the interferometric detection. The beam was expanded and collimated with a telescope that was adjusted using a shear plate to optimize collimation. The divergence was measured to be 0.03°. The beam was set to be incident on the substrate at an angle near the expected reflectivity minimum (∼70.9°) with a polarizer in the beam path to enforce s-polarization. The substrate was rotated to adjust the incidence angle for minimum reflectivity. The reflected light was detected by a photomultiplier tube covered with a 75-μm-diameter aperture that determined the spatial resolution of the experiment. The probe laser was mechanically chopped, and phase-sensitive detection was used for convenience so that rigorous elimination of stray light in the laboratory was not necessary. The substrate was moved using a computer-controlled stepping motor assembly capable of two-dimensional translation so that a reflectivity map could be generated. The step size in the direction orthogonal to the beam propagation direction was adjusted to be approximately commensurate with the pinhole size to preserve the spatial resolution allowed by the pinhole, and the reflectivity at each point was measured with a 100-ms time constant after waiting 300 ms for the value to settle at a new point. Step sizes were chosen to be ∼2.7 (= tan(70.9°)) times larger in the direction along the beam propagation direction since the resolution in that direction is degraded by the oblique angle of incidence. An area of approximately 0.3 cm × 0.3 cm could be scanned in less than 7 min. Note that the method can also be implemented with a camera as the detector to accelerate detection but that signal-to-noise ratios are slightly reduced in that case. Camera images are complicated by interference since the laser is coherent and by diffraction from the array spots. Also, the dynamic range of a typical CCD camera is much less than that of a photodiode or photomultiplier tube.

Wavelength Scanning RI Measurement. Verification that we can quantitatively determine the amount of material detected using single-color RI requires an independent measurement of the amount of biotin and streptavidin deposited on our chips using the chemistry outlined above. Therefore, two-spot chips were made using identical chemistry where one spot has biotin and the other biotin bond plus streptavidin. Interference coating thicknesses at the spot locations were measured by wavelength scanning RI (ws-RI) in an apparatus where the wavelength could be tuned to map out the substrate topology. The optical apparatus and data analysis procedures for ws-RI have been described in previous literature.[12]

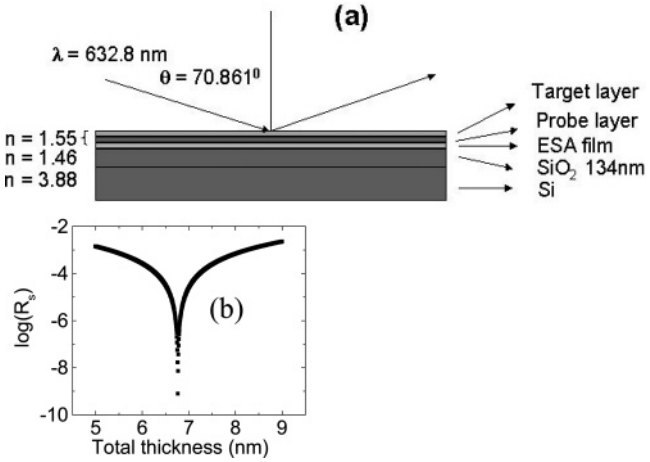

Figure 2. (a) Geometry used to model reflective interferometry where λ is the incident wavelength used to probe the structure and θ is the incident angle. The silicon substrate is coated with a thick oxide, which is in turn coated with self-assembled polyelectrolyte bilayers, a probe layer, and a target layer. The polyelectrolytes, probe, and target are all assumed to have refractive indeces of 1.55 while literature values are used for the other materials. (b) Transfer matrix computation of the structure reflectivity versus the total thickness of the layers above SiO_2. The probe wavelength is 632.8 nm, the incidence angle is 70.861°, and there is a 134-nm-thick oxide.

RESULTS AND DISCUSSION

Theoretical Modeling of Single-Color RI with Ideal Geometry. Figure 2a illustrates the layer model we use to compute reflectivity. The refractive indexes of the silicon and silicon oxide are taken from the literature while all of the organic components including the polyelectrolytes, biotin, and streptavidin are taken to have refractive indexes of 1.55. A transfer matrix formalism is applied to compute reflectivity for s-polarized incident light. The conditions closest to complete destructive interference are achieved when the light source is strictly monochromatic and perfectly collimated, and the substrate coating is completely uniform with thickness determined by the probe wavelength. Figure 2b plots absolute reflectivity versus total thickness of the organic components where the wavelength is taken to be monochromatic (632.8 nm), the oxide thickness to be 134 nm, and we assume perfect collimation and layer uniformity. As with other methods based on reflection such as surface plasmon resonance, the figure of merit for detection is the ratio of reflectivity with target binding relative to that without it. The extremely deep minimum allows for that figure of merit to be extremely high in principle, much higher than that achievable for SPR. For example, the data of Figure 2b suggest that a 2-Å increase in coating thickness (e.g., due to target binding) can produce as much as a 4 order of magnitude increase in reflectivity. In this particular implementation of RI, the fundamental limitation has to do with the fact that the refractive index of the silicon substrate is complex due to absorption above its indirect band gap. With a nonzero absorptive part of the refractive index, perfect destructive interference cannot be achieved. Longer wavelengths will exhibit deeper minimums as one probes further from the direct band gap of the substrate.

In practice, limitations on the achievable sensitivity using RI come from nonideal conditions including finite spectral bandwidth and angular divergence of the light source as well as inhomogeneity and roughness of the overlayers on the substrate. For the implementation here with a source of light that is not tunable, the absolute thickness of the overlayers is also critical in maximizing the reflectivity contrast between regions of slightly different thickness. We define reflectivity contrast at a given position on the substrate to be $1 + \Delta R/R_0$, where ΔR is the increased reflectivity relative to that measured in a reference region, R_0. Figure 2b illustrates clearly that a strategy to fine-tune the overlayer thickness is necessary to achieve optimal results with single-color RI and is the motivation for developing layer-by-layer assembly to augment thermally grown oxides.

Theory of Practical Single-Color RI and Comparison with SPR. Detailed modeling of how the reflectivity contrast is degraded when the conditions for RI are nonideal is included in the Supporting Information. In particular, we model how the sensitivity of RI is degraded when the interference layer thickness is not optimal for the probe wavelength as well as how the sensitivity is decreased when there is finite source bandwidth, finite angular divergence, and spatial inhomogeneity in the interference layer thickness. We also model "ideal SPR", where SPR is performed under literature conditions with a source that has perfect bandwidth and collimation and a substrate with the optimal thickness of gold and no chromium or titanium adhesion layer. Briefly, we find that 1 nm of target adsorption doubles the reflectivity in SPR while, even for realistic conditions (0.03° angular divergence and 1-nm-thickness inhomogenity in the interference layer), the reflectivity would increase by a factor of ~15 in RI. This factor is reduced to ~5 if the interference layer is also fabricated 0.5 nm too thick. Thus, we conclude that RI is superior to ideal SPR even for nonidealities considerably worse than what is realistically achievable. It is worth noting, as is clear from thinking about Figure 2, that thickness inhomogeneity in the interference layer means that it is much better for a substrate to be slightly too thick than for it to be slightly too thin in order to achieve best reflectivity contrast.

LBL ESA Results. As is clear from the modeling in Figure 2, it is critical to modify the thickness of the interference coating to be precisely correct. Commercially available Si/SiO_2 wafers have thermally deposited SiO_2 layers generally only accurate to within a few nanometers (±3−5% of the oxide thickness). Our strategy was to buy substrates substantially thinner than ideal for 632.8-nm destructive interference and to augment the film to the desired thickness using LBL ESA.

Deposition thicknesses obtained using LBL ESA were assessed on silicon wafers using spectroscopic ellipsometry. Figure 3 presents thickness data versus the number of bilayers of PAH and SPS deposited where the error bars represent reproducibility over several deposition runs, typically better than 0.5 nm.

We use PAA as a final layer so that its carboxylic acid groups are available for probe attachment and assume its thickness is the same as that for SPS as measured in Figure 3. The experimental data are well fit by a linear relationship between number of bilayers and thickness so that we can control the film growth and augment an oxide of measured thickness by the correct number of bilayers to compensate for variations in the thickness of the thermal oxide grown on the silicon wafer.

We used three substrates with oxide thicknesses between 134 and 137 nm and augmented them with LBL ESA by 6, 7, and 8 bilayers. The idea behind using three substrates was to deliber-

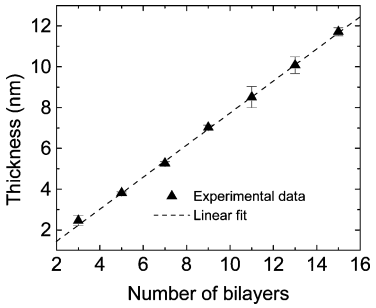

Figure 3. Ellipsometrically determined thickness of electrostatically assembled polyelectrolytes versus the number of deposited bilayers. Triangles denote values averaged over several runs while the error bars represent the standard deviation between runs. A linear fit to the data is shown as a dashed line.

ately create experimental circumstances corresponding approximately to the cases considered in the Suuporting Information, where a substrate could be nearly exactly correct for destructive interference or too thin or too thick by ~0.5 nm. Ellipsometric measurement of the substrates before and after LBL ESA gave us values of thickness for the three interference layers that had 0.69 nm too little polymer, nearly exactly the correct polymer thickness, and 0.14 nm too much polymer before application of biotin or streptavidin.

Biomolecular Detection Results. Four-spot chips were made from these three substrates by the procedure described in the Experimental Section. Figure 4 shows the single-color RI contrast images of the three chips. The reflectivity contrast $1 + \Delta R/R_0$ is plotted where R_0 is the reflectivity of the background as measured by the average reflection from a corner of the sample far from the treated spots. The gray scale for contrast values is shown on the right side. The contrast images indicate that when the substrate thickness is exactly perfect, the reflectivity contrast $1 + \Delta R/R_0$ for streptavidin-treated regions with respect to the background averages 76 over the spots (Figure 4b, spots 1 and 2) with places where the contrast is over 100. For the biotin-only spot, the contrast is 17 (Figure 4b, spot 3), and for the nonspecific binding of streptavidin on polyelectrolytes without biotin, a contrast of 5 (Figure 4b, spot 4) was observed. When the thickness is a little thinner or thicker, the streptavidin binding contrast decreased to 19 (Figure 4a, spots 1 and 2) and 37 (Figure 4c, spots 1 and 2), respectively, with much smaller changes in the control spot 4. It is interesting to note that biotin appears to be more easily observed on the chip that is slightly too thick. The reason for this has to do with the roughness (thickness inhomogeneity on length scales less than the instrument resolution of ~100 μm) being larger than the biotin thickness such that more regions of the chip with precise average thickness have regions that are too thin and contribute reflectivity contrast less than unity to the overall observed signal.

Quantitative Comparison with Theory. Determining whether the reflectivity contrasts we observe agree with the theoretical prediction based on optical theory is tantamount to assessing whether single-color RI can be used to derive quantitative results for the amount of adsorbed material. We know the interference coating (background) thickness without probe or target from ellipsometry, the HeNe wavelength, and have measured the probe beam's angular divergence (0.03°). For a full comparison of the data of Figure 4 with theory, we also need independent measurements of the amount of biotin and streptavidin bound to the spots and of the surface inhomogeneity. To determine the amount of biotin and streptavidin attached to the spots, we used wavelength scanning reflective interferometry since thicknesses are easily extracted. To determine surface inhomogeneity, we measured the ratio of p-polarized reflection to s-polarized reflection for the substrate with oxide only and assumed that the polyelectrolyte layers were approximately conformal. The p-polarized reflectivity is ~20% and insensitive to interference layer thickness so that it can be used to calibrate the absolute s-polarized reflectivity of the substrate. When the oxide thickness is known from ellipsometry and the angular divergence is measured, the coating thickness inhomogeneity can be extracted from the theory. This involves calculating the predicted s-reflectivity with the experimentally determined angular divergence and interference layer thickness for various thickness inhomogeneities and finding the one that matches the experimentally determined s-reflectivity.

Biotin and Streptavidin Thickness Determination. Figure 5a shows a schematic of a two-spot structure created on a control Si/SiO_2 substrate. Identical chemistry was applied to what was used for spot 3 (biotin only) and spot 1 (biotin and streptavidin) of the experimental substrates discussed previously. After LBL ESA, 1.0-μL droplets of biotin solution were applied to both spots 1 and 2 of the control substrate. Spot 2 was further exposed to the streptavidin solution, followed by thorough water rinsing and drying under flowing nitrogen gas. Figure 5b presents raw data of reflected intensity versus wavelength derived from three different spatial regions on the chip that represent background, the biotinylated spot, and the spot containing both biotin and streptavidin. The minimum reflectivity in those three regions can be derived from fitting to a parabola and occurs at 633.7, 635.7, and 646.7 nm, respectively. The topology is extracted from theory using a transfer matrix model and illustrated in Figure 5c. We assumed that the refractive index of the biotin and streptavidin layers is 1.55, typical for organic materials far from resonance, and found that the average deposition of biotin in its spot was 3.5 $\pm$ 0.5 Å and streptavidin plus biotin in its spot was 26.5 $\pm$ 0.5 Å. Since the technique measures optical phase delays that are proportional to the product of path length traveled in a material and its refractive index, if our assumed refractive indexes are too low (high) by a few percent then our inferred adsorption thicknesses will be too high (low) by a few percent. Notice that the best reflectivity contrast between the streptavidin and biotin spots is around 5−6 when the biotin spot is close to its minimum reflectivity. Because the probe light is from a lamp and spectrometer, its bandwidth and collimation are poor relative to the laser used for single-color RI and so the contrast is correspondingly much worse than for laser probing as reported in the present paper.

Coating Thickness Inhomogeneity Determination. To estimate the coating thickness inhomogeneity, we measured the reflectivity ratio of p-polarized light versus that of s-polarized light from a bare wafer to determine the absolute s-reflectivity and compared with theory using inhomogeneity as the only adjustable parameter. With this procedure, we determined the inhomogeneity in the interference layer thickness to be 1.28 nm, a value consistent with AFM profiles of selected spots on our wafers. We assumed

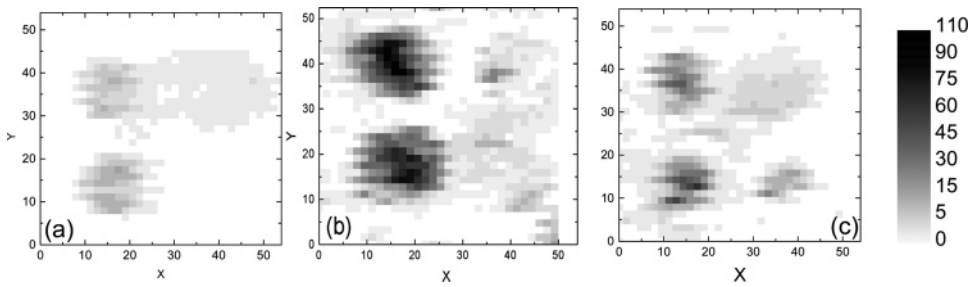

Figure 4. Reflectivity contrast maps of three treated substrates with spots oriented as in Figure 1. The scanned area is approximately 3 mm × 3 mm. The gray scale at the right conveys the reflectivity contrast $1 + \Delta R/R_0$, where R_0 is the reflectivity in an untreated corner of the substrate. Three different substrates that underwent identical chemical treatment as described in the text are scanned: (a) ~0.69 nm too thin; (b) nearly the correct thickness; (c) ~0.14 nm too thick.

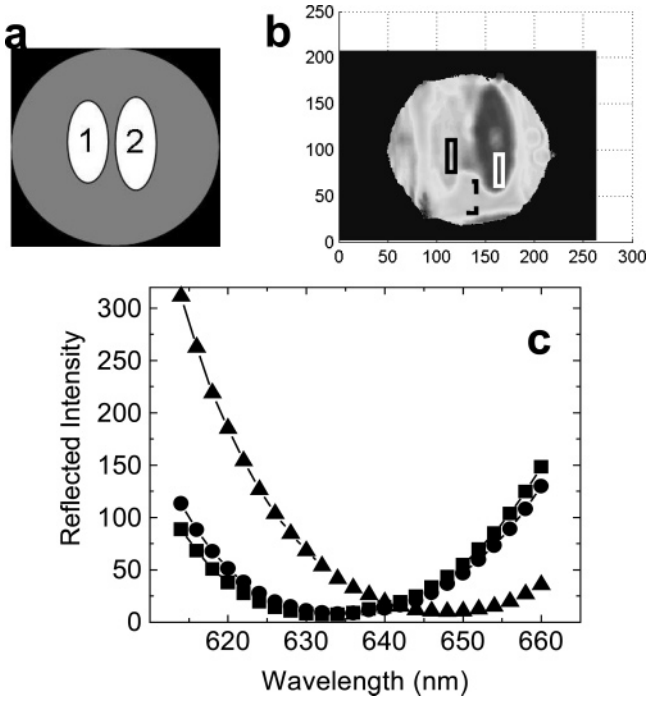

Figure 5. Wavelength scanning interferometry to determine biotin and streptavidin layer thicknesses. The experiment is done on a wafer with layers such as those of Figure 2. (a) Spot geometry with the left spot having only biotin applied and the right spot having biotin followed by streptavidin. (b) Raw data on reflection versus wavelength and fits for reflectivity in the labeled rectangular regions encompassed by the background (squares), biotin (circles), and biotin/streptavidin (triangles). The curves are compiled by extracting data from reflection taken at various wavelengths with a CCD camera.

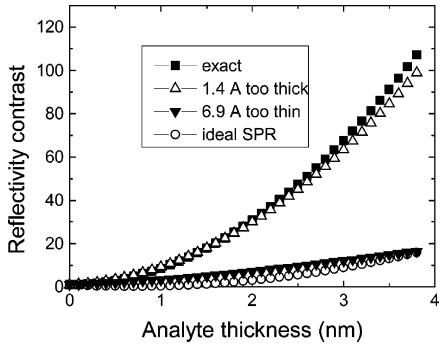

Figure 6. Theoretical curves for reflectivity contrast $1 + \Delta R/R_0$ versus analyte thickness on each of the three substrates measured in Figure 4. The modeling uses the ellipsometrically measured interference layer thicknesses and the measured experimental parameters for angular divergence (0.03°) and inhomogeneity (1.28 nm). For comparison, the contrast for SPR with ideal thicknesses and no divergence or inhomogeneity is plotted using a literature geometry from ref 16 (see Supporting Information).

that the inhomogeneity of each of the wafers we used was the same and that the polymer bilayers are conformal and do not change the inhomogeneity.

Comparison with Theory. Using this value of inhomogeneity, we calculated theoretical curves of $1 + \Delta R/R$ versus target thickness for our three substrates using the measured thickness, probe beam divergence, and no adjustable parameters. Those results are plotted in Figure 6 and should be directly comparable to the experimental results in Figure 4. The predicted contrast for the streptavidin spots are 9, 53, and 50 for the substrates used, assuming combined deposition of 2.65-nm biotin plus streptavidin. These correspond reasonably well with the experimental results of 17, 76, and 37. The approximate agreement implies that semiquantitative conclusions regarding amount of target binding can be made from single-color RI measurements. More important, it confirms our conclusion that spatial inhomogeneity of the coating thickness is the present limitation on the sensitivity of the method. That sensitivity could reasonably be expected to improve by almost another order of magnitude with a smoother oxide (cf. Supporting Information). Nevertheless, ideal SPR has contrast of only 10 for 3-nm adsorbed material.

The contrast values we measure for biotin are a factor of ~2 better than predicted by our theory for the correct thickness interference layer. This discrepancy may arise since we have treated thickness inhomogeneity as a flat distribution for computational convenience rather than a more realistic distribution such as a Gaussian. For very small adsorbate thickness (i.e., less than the inhomogeneity in the coating thickness) on substrates with nearly exact average thickness of the interference layer, the detailed assumptions one makes about the inhomogeneity distribution strongly affect the reflectivity result.

Evaluation of Detection Sensitivity. We can also estimate the minimum detectable amount of analyte in a practical implementation of single-color RI from Figure 6. Of particular importance is how well we can determine the average reflectivity contrast over a spot. Assuming Gaussian statistics, if we sample N pixels in the spot, the error in the average reflectivity contrast will be the square root of the variance divided by the number of points sampled, $(\sigma^2/N)^{1/2}$. Using these values in Figure 4b, a randomly chosen region of the background gives reflectivity contrast $1 + \Delta R/R = 1.08 \pm 0.28$. Taking two standard deviation changes in the average as a measure of what we could realistically

detect, we would need reflectivity contrast greater than 1.56 before we could say with confidence that additional adsorption had occurred on the wafer. Combining this value with the theory of Figure 6 implies minimum detection limits of 1.2 Å of material. The situation when looking at adsorption on areas other than the background (e.g., streptavidin target on biotin probe spots) is more complex since we also need to allow for spot-to-spot variations in the amount of bound probe. A similar analysis of the biotin spot gives an average reflectivity contrast of 10.5 ± 0.4. Conservatively, we could be confident that target adsorption has occurred if the average reflectivity contrast increased to 15, and this also leads to the conclusion that we could detect ~1 Å binding of streptavidin. One nice consistency check on the validity of this approach to estimating the minimum thickness we could detect is that the two distinct experimental spots where we applied streptavidin have consistent reflectivity contrasts, measuring 45.3 ± 2.2 and 44.7 ± 2.8, respectively.

Biomolecular detection sensitivities are frequently reported in units of picograms per milliliter, and it is interesting to consider the potential detection sensitivity in these units when 1.2 Å (120 pm) average adsorption is observable. We assume here that binding constants are high so that analyte present in the fluid will bind to the surface. Taking a 1-mm spot, typical for spots sizes made by application of 1-μL quantities of solutions for probe attachment, the volume occupied by adsorbates (1 mm × 1 mm × 120 pm) would be $\sim 1.2 \times 10^{-12}$ cm^3. With a density of 0.7 g/cm^3, this would mean 0.8 pg of adsorbed material can be detected. Assuming that 1 μL of analyte is applied, the sensitivity of single-color RI would translate to 0.32 pg/mL. We prefer to quote the sensitivity in terms of detectable average adsorbate thickness since this makes no assumptions about spot geometries or analyte volumes and is therefore directly comparable to theory and SPR.

CONCLUSIONS AND FUTURE WORK

We have developed and refined a simple method for measurement of molecular binding at interfaces using reflective interferometry where only a single-color probe source is required. We have implemented the approach using thermal oxides on silicon since they are very flat and easy to obtain. Silicon also has the advantage of being very weakly absorbing in the visible below its direct band gap so that near perfect destructive interference can be obtained. At the same time, silicon is opaque to visible light so that complications due to backside substrate reflections are avoided. Because the thickness of the antireflection coating is critical when the excitation source is not tunable, we have shown that augmenting the thickness using layer-by-layer electrostatic assembly of polyelectrolytes can be done to make the interference coating thickness nearly ideal for a given probe wavelength. Moreover, poly(acrylic acid) presents useful carboxylic acid groups that can be used to functionalize the surface with molecularly specific probes such as biotin through condensation chemistry. Alternate approaches to tailoring coating thickness such as controlled HF etching of the oxide are also viable.[19]

Using a laser to probe the surface allows for highly collimated and monochromatic light so that high sensitivity can be achieved. In fact, we are able to see increases in reflectivity of 2 orders of magnitude due to binding of a 3-nm layer of biomolecules on the surface. This contrast is much better than what can be done with surface plasmon resonance. Our present minimum detectable level of adsorption is less than 0.12 nm, which, for perspective, would correspond to roughly 2% monolayer of a typical 20-base-long DNA oligonucleotide. Further improvements seem likely with flatter oxide coatings on the silicon wafers. Theoretical RI has an enormous advantage over SPR in dynamic range and sensitivity due to the depth of the reflectivity minimum near conditions of perfect destructive interference. While practical single-color RI cannot approach the theoretical limit, it nevertheless promises to be at least 1 order of magnitude more sensitive than SPR although single-color RI is simpler to implement.

We have shown that the amount of adsorption can be determined semiquantitatively once three experimental parameters are measured, the angular divergence of the laser, the inhomogeneity of the coating thickness, and the absolute coating thickness. The first is measured directly, the second by polarized reflectivity, and the third by ellipsometry. Using these as inputs to a transfer matrix theory of the reflectivity, the amount of material deposited inferred from reflectivity contrast agreed well with what was measured independently using wavelength scanning reflective interferometry.

While many detection chemistries are sufficiently robust to withstand rinsing and drying,[20] adaptation of RI to working at interfaces in aqueous environments is of obvious importance for biomolecular sensing. Theoretical results for model geometries under water are very close to those under air. Physically, the close correspondence is easy to understand because the degree of destructive interference depends primarily on the path length difference between waves reflected at the interface between air or water and the oxide and waves reflected at the oxide/silicon interface. The main difference in the case of water is that the incidence angle for the light onto the substrate must be steeper to maintain balance in magnitude between the reflections from those two interfaces. The modification to probe under aqueous media is straightforward to implement and has been discussed previously.[12]

ACKNOWLEDGMENT

We are grateful to the Infotonics Center of Excellence for initial support of this project and to Dr. Alan Raisanen at the Rochester Institute of Technology for growth of the thermal oxides. Prof. Michael Rubner and his research group kindly helped to teach us how to do layer-by-layer electrostatic self-assembly and shared their automation software with us. We also thank Charlie Mace and Ben Miller for useful discussions and sharing their results prior to publication.

SUPPORTING INFORMATION AVAILABLE

Modeling of nonideal single-color RI including effects of probe source bandwidth, probe divergence, interference layer thickness mismatch, and inhomogeneity. This material is available free of charge via the Internet at http://pubs.acs.org.

(19) Mace, C. R.; Striemer, C. C.; Miller, B. L. *Anal. Chem.* **2006**, *78*, 5578−5583.

(20) Friedman, B.; Gaspar, M. A.; Kalachikov, S.; Lee, K.; Levicky, R.; Shen, G.; Yoo, H. *J. Am. Chem. Soc.* **2005**, *127*, 9666−9667.

Received for review May 18, 2006. Accepted July 17, 2006.

AC0609226